Optimization of Multi-Junction Solar Cells for the Martian Orbit

Jéssica O. Lorenzi
Department of Physics
CEFET/RJ
Petrópolis, Brazil
jessica.lorenzi@outlook.com.br

Daniel N. Micha
Department of Physics
CEFET/RJ
Petrópolis, Brazil
ORCID: 0000-0003-0572-7367

***Abstract*— Photovoltaic (PV) devices have been used in space applications since 1958, and since then, missions to space have placed increasing demands on the power supply systems. Orbital and surface exploration missions are planned to Mars for the decade 2023-2032 by the National Aeronautics and Space Administration (NASA). Considering that space applications require power systems with high specific power (W/Kg), it is crucial to know the optimized device configuration for these environments for PV to become a viable option. The objective of this work is to present the optimal bandgap energy configuration for cells of different number of junctions operating at the Martian orbit. For this, blackbody modeling was used to obtain the extra-Martian solar spectrum and, by means of a computer simulation based on the Schockley-Queisser detailed balance model, the optimal bandgap energy combination is obtained for each configuration. As results, we obtained for the best double junction solar cell an efficiency of 45.3% with bandgaps of 0.90/1.60 eV and 51.7% for triple junction solar cell with 0.75/1.22/1.84 eV.**

Keywords*— *Space Application; Multi Junction Solar Cells; Efficiency; Mars.

I. INTRODUCTION

Photovoltaic (PV) solar cells for space applications have a constraint of delivering a high specific power (W/kg) in order to decrease the launch cost of satellites and other PV driven space gadgets [1]. Ge/InGaAs/InGaP 3JSC (triple junction solar cells), with a bandgap energy (E_G) combination of 0.67/1.4/1.85 eV, are the standard device for space application which presents an efficiency of about 35% under the extraterrestrial AM0 spectrum [2,3]. Nonetheless, it has been shown that its specific power can be improved by using other material combinations that make better use of the solar spectrum [4] or other fabrication techniques that allow for weight reduction [5].

New space missions have their specific characteristics and needs for power supply systems. A report published by NASA in 2017 discusses the solar power technologies for future planetary science missions analyzing the existent solar cell in the market at that time and pointing out the main optimization needed for further improvement [2]. Mars is listed as one important environment in which PV power systems will be used still in this decade. However, according to the document, there are challenges to be overcome if one wants to stick to the existent PV technology to supply power under the Martian environment. In general, beyond stressing the need for specific power enhancement, they discuss that missions on the surface will need much more technology development, as Mars offers a very harsh environment. First, the solar cells will need to operate much more efficiently under the Martian spectrum itself. In addition, the frequent sandstorms shall be considered, as they create shadowing and soiling, reducing the access of the PV arrays to the sun [2].

The Mars Optimized Solar Cell Technology (MOST) NASA project [6] was successful in theoretically determining the solar spectrum on the Martian surface for two different latitudes and in creating optical simulators to be used for solar cell characterization on Earth. Therefore, Spectrolab and Emcore were able to present optimizations on their Ge/InGaAs/InGaP 3JSC to operate more effectively under the modeled spectrum of the Martian surface. The optimized cells were tested and showed significant gains in performance [6,7]. However, all the optimization work was based on the structure of existing cells and no other new one was proposed. Furthermore, only the spectra for the surface of Mars were considered.

This work aims to investigate the optimal configuration of E_G to be used in 2JSC and 3JSC under the Martian orbital spectra using detailed balance modelling. Such spectra were obtained using radiometric laws considering the sun as a blackbody radiator and the Martian orbital parameters.

II. METHODOLOGY

A. Modelling of the extra-Martian solar spectra

Planck's law for the emission of black body radiation is used to describe the sun' spectral irradiance I_λ per solid angle [$W.m^{-2}.sr^{-1}.nm^{-1}$]. The total irradiance I arriving at a point on the Martian surface (disregarding the atmosphere) oriented with a zenithal normal angle θ can be obtained by integrating I_λ over the wavelength and the solid angle Ω, as in the first equality of eq. (1):

$$I(T,\lambda,d) = \int_\lambda \int_\Omega I_\lambda \cos\theta \, d\Omega d\lambda = \frac{\pi R_S^2}{d^2} \int_0^\infty \frac{2hc^2}{\lambda^5\left(e^{\frac{hc}{\lambda kT}}-1\right)} d\lambda \quad (1)$$

Using the radiance theorem [8], I can be equivalently calculated using the Martian's viewpoint and I_λ at the point of emission. Considering the great distance d between Mars and the sun, θ = 0 can be considered constant. Thus, the integration over Ω yields the total solid angle subtending the sun from Mars, which on its turn depends on the sun's radius R_S and d. These considerations result in the second equality in eq. (1), in which h is the Planck's constant, c is the speed of light, k is the Boltzmann constant, and T is the sun temperature.

Figure 1 shows the spectral irradiance (I_λ integrated over Ω) obtained for the perihelion, aphelion and the mean distance of the Earth's and Mars' orbits, using eq. (1) with T=5775K and the distances shown in Table 1.

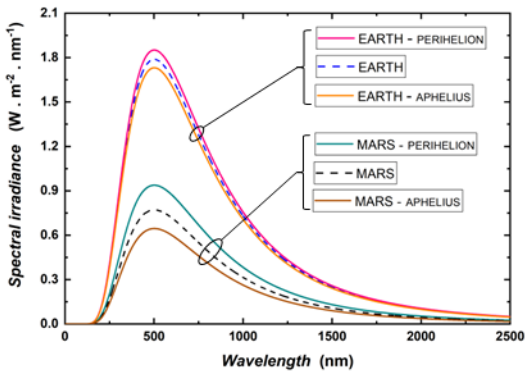

Fig. 1. Solar spectral irradiance obtained for Earth and Mars at different orbital points using radiometric modeling.

The total irradiances found for such points of the Earth's and Mars' orbits are also shown in Table 1. The values for the mean orbital distances were used to find the mean total irradiance $\langle I \rangle$ and validate the model by comparing to data provided by NASA: 1361 W/m^2 and 586 W/m^2, respectively [9, 10], which are in good agreement to our results (< 0.3%).

From Figure 1, one can notice the larger difference between the aphelion and perihelion irradiances on Mars in comparison to the ones on Earth. This is due to the different orbit eccentricities, which is much less pronounced in the case of the Earth. In addition, it is possible to see that all the spectra have a common peak, which depends only on the temperature of the sun. Table 1 shows that from perihelion to aphelion, I has an increase of 45% for Mars whereas for the Earth this difference is of only 3.4%.

Table 1. Distances and total solar irradiances for the aphelion, perihelion and the mean orbital distance of Earth and Mars.

Planet	Orbital point	Distance (10^6 km)	I (W/m^2)
Earth	Aphelion	152.1	1314
	Perihelion	147.1	1405
	Mean	149.6	1358
Mars	Aphelion	249.2	489
	Perihelion	206.6	712
	Mean	227.9	585

B. *Multijunction solar cell efficiency calculation*

Multijunction solar cell efficiency was calculated using the detailed balance model having as input the solar spectrum calculated according to section II.A, the solar cell temperature T_C and the bandgap energies E_G^{Ji} of the junctions, in which i is the junction index counted from the bottom upwards. The E_G values are for the local conditions and cannot be directly compared with the known ones for the materials on Earth. To make this correspondence, it is necessary to use the material's Varshni parameters. The methodology for the calculations was the same as in [4] in which current-voltage (IV) curves are simulated from which the figures of merit, such as the efficiency, are extracted. T_C for a flat plate in the Mars' orbit was calculated using the thermal equilibrium condition between the solar radiation and the cell emission, which results in T_C = 225 K.

The efficiencies under the extraterrestrial solar spectrum were obtained and used for validation by comparison with data from literature (for which good agreement was obtained, not shown here). Then, the extra-Martian spectra were used in the simulations to generate the results presented in the next section. The fine E_G variation was 0.01 eV.

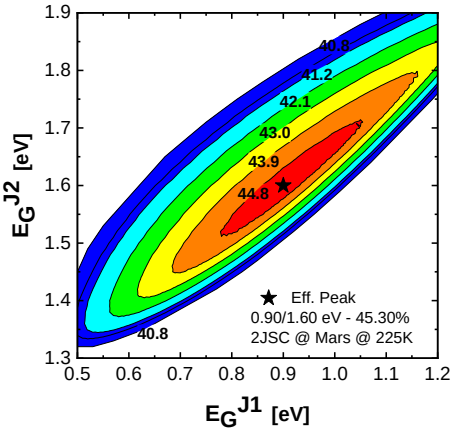

Fig. 2. Color map of the 2JSC efficiency under the mean distance extra-Martian solar spectrum as a function of the bandgap energies of the junctions.

III. Results and Discussions

A. *2JSC efficiency under extra-Martian spectrum*

Figure 2 shows a color map of the 2JSC efficiencies under the mean distance extra-Martian solar spectrum as a function of the E_G of the junctions at T_C = 225 K. The results for the aphelion and perihelion are not shown and are only shifted by a small difference in the efficiencies in comparison to the ones shown in Figure 2.

From Figure 2, one can see that the efficiency peak is reached at 45.3% for E_G^{J1}/E_G^{J2} = 0.9/1.6 eV. This value is higher than the one shown by the optimum solar cell for the extraterrestrial spectrum (T_C = 298 K), namely 41.6% for a very similar combination E_G^{J1}/E_G^{J2} = 0.98/1.66 eV (see Table 2). At the Mars orbital environment, the solar cell is under a spectrum which is $C = \frac{\langle I_{Mars} \rangle}{\langle I_{Earth} \rangle} = 0.43$ times less intense than the one at Earth and at a temperature 73 K lower. The open-circuit voltage (V_{OC}) of the two cells is very similar, and so is the fill factor (FF). At lower temperatures, a higher V_{OC} would be expected for a given E_G configuration due to less radiation emission. However, as the best 2JSC for the two planets are different, the higher E_G values for the 2JSC on Earth compensates for the thermal loss. Therefore, the difference in efficiency resides in the short-circuit current density (J_{SC}), optimized when current matching takes place amongst the junctions. The J_{SC} ratio for the two best devices is 0.46, a value higher that C, finally explaining the difference in efficiency. Noteworthy is the fact that the combination with the same E_G as the one for Earth reaches a very high efficiency (45.2%) and for this device, the expected behaviors of J_{SC} (ratio = 0.43) and V_{OC} are attained (see Table 2).

Table 2. Figures of merit for the best 2JSC working under the Earth and Mars orbital conditions.

Planet	E_G^{J1}/E_G^{J2}(eV)	J_{SC} (mA/cm^2)	V_{OC} (V)	FF	$Eff.$ (%)
Earth	0.98/1.66	29.62	2.07	0.90	41.6
Mars	0.90/1.60	13.68	2.07	0.91	45.3
Mars	0.98/1.66	12.76	2.19	0.92	45.2

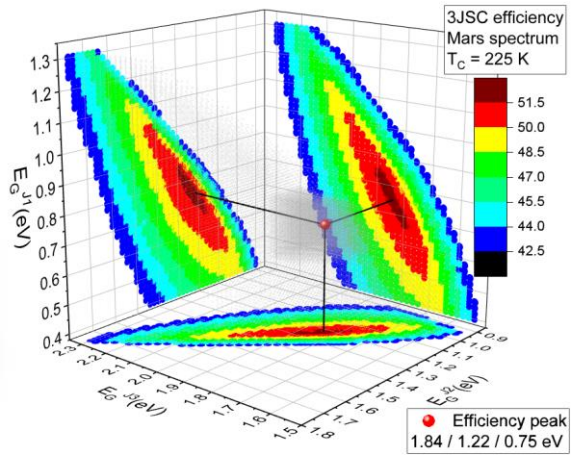

Fig. 3. Mapping of efficiencies as a function of bandgap energies for 3JSC under the Mars orbital solar spectrum.

Furthermore, one can see in Figure 2 that there is a large E_G region showing high efficiencies. The colored region inside the blue area leads to efficiencies higher than 40.8% and the one in dark red is for values higher than 44.8%. This shows that several material combinations can be used to attain the needs of high efficiency in the power supply of missions in the extra-Martian orbit when using a 2JSC.

B. 3JSC under extra-Martian spectrum

Figure 3 presents the results for the efficiency of 3JSC under the mean distance extra-Martian solar spectrum as a function of the E_G of the junctions. The points in the 3D representation (transparent gray shaded region) are only for efficiencies higher than 42.5% and the colored projections in the planes facilitate the reading of the efficiency of the respective E_G combinations.

In Figure 3, the peak is for the combination 0.75/1.22/1.84 eV reaching an efficiency of 51.7%, an absolute gain of 6.4% compared to 2JSC. As for 2JSC, there is an efficiency increase in comparison to the optimum cell working under the extra-terrestrial AM0 spectrum of 46.5% (obtained for 0.77/1.21/1.84 eV), which can be again explained by the differences in the total irradiance arriving at the Martian orbit and the different T_C. We again observe that several E_G combinations lead to very high efficiencies under operation in Mars. Noteworthy, the standard 3JSC used for space applications, namely Ge/InGaAs/InGaP, with a E_G combination of 0.69/1.44/1.90 eV under T_C = 225 K (Varshni parameters given in [12]) is not one of them. It shows a low efficiency of 38.3%.

In Figure 4, we further analyze the operation of the standard 3JSC under Mars conditions by showing the *IV* curves for the full device (dashed) and the ones that would be obtained by each junction if they were submitted to the filtered spectral that they receive after the sunlight has passed through the top junctions (solid lines). In this case, the Ge junction (J1) absorbs much more photons than J2, generating a virtual J_{SC}^{J1} of 16.3 mA/cm^2 versus a J_{SC}^{J2} of 6.85 mA/cm^2. A way to overcome current mismatch still keeping the same materials would be by working with the junctions' thicknesses or exploring junctions' luminescence coupling [11], but in this case, it is not possible as the Ge junction is the bottommost junction.

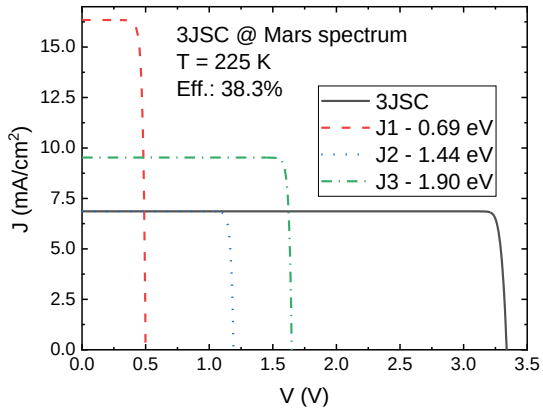

Fig. 4. *IV* curves of the standard Ge/InGaAs/InGaP 3JSC illuminated with the Martian orbital solar spectrum and T_C = 225 K.

Figure 5 presents the IV curves for the optimized 3JSC both for the Mars (solid lines) and the extraterrestrial (dashed lines) solar spectra along with the virtual curves for the individual junctions. First, one can notice the good current matching among the cells shown by both combinations. The V_{OC} for the 3JSC in Mars is higher, as expected. Table 3 summarizes the figures of merit for both 3JSC.

IV. Conclusions

In this work, we investigated the best MJSC configuration for PV operation in the Mars' orbit. First, we obtained the extraplanetary spectra for the Earth and Mars by modeling the sun as a blackbody at a temperature of 5775K and using radiometric laws to the planet's orbit. The resulting total irradiances were very close to the tabulated values in literature. Using such spectra as input and the local temperature, we simulated the efficiency of several MJSC with two and three junctions and found the optimal E_G combinations for both configurations. The optimal 2JSC for use in the Martian's orbit shows 45.3% for 0.9/1.6 eV. This would represent a maximum electrical power density supply of 265 W/m^2 considering the planet's mean distance to the sun. Comparing to the best 2JSC working in the extraterrestrial environment that can deliver 565 W/m^2 (efficiency of 41.6% and irradiance of 1358 W/m^2), PV modules 47% larger in area shall be used in Mars. If one considers the differences in irradiances in the Martian orbit of +21.6% for the perihelion and –16.3% for the aphelion, a further PV module area increase must be considered in the project to keep a constant power supply to the batteries. For 3JSC, the optimal bandgap combination is 0.75/1.22/1.84 eV for Mars reaching an efficiency of 51.7%. The power density supply of PV modules composed by such solar cells would be 6.4% higher in absolute than the ones discussed for 2JSC.

The optimal E_G combination found with the simulations for 3JSC differs strongly from the one shown by the standard device used for space applications, namely Ge/InGaAs/InGaP. By analyzing the IV curves of both combinations, it was possible to show that the standard 3JSC presents a

Table 3. Figures of merit for the best 3JSC working under the Earth (E) and the Mars (*M*) orbital conditions.

	$E_G^{J1}/E_G^{J2}/E_G^{J3}$ (eV)	J_{SC} (mA/cm^2)	V_{OC} (V)	*FF*	*Eff. (%)*
E	0.77/1.21/1.84	23.18	2.95	0.90	46.5
M	0.75/1.22/1.84	10.27	3.13	0.92	51.7

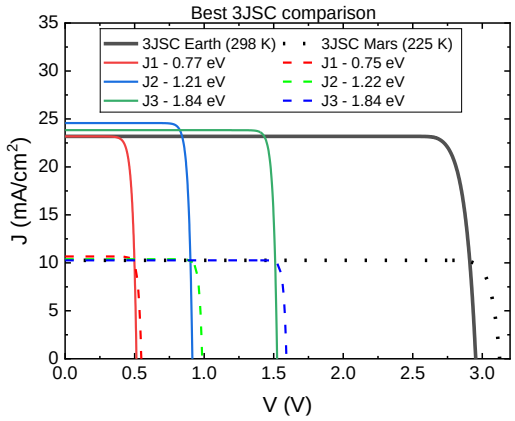

Fig. 5. *IV* curves of the best 3JSC under the Earth and Mars orbital conditions.

performance 26% lower than the optimum case, especially due to a mismatched J_{SC}, which in the case of the best device shows a matched value of around 10 mA/cm^2 against 6.85 mA/cm^2 for the standard 3JSC.

As a perspective, we intend to extrapolate our model to study the optimum PV MJSC for other planets and to the Martian's surface. Moreover, in possession of the efficiency charts, we aim to generate a list of suitable materials to reach high efficiencies under the next planned extraplanetary missions in order to contribute to space exploration.

ACKNOWLEDGMENT

This work was partially funded by CNPq. DM is now with III-V Lab, Nokia Bell Labs France.

REFERENCES

[1] A. Luque and S. Hegedus, Handbook of Photovoltaic Science and Engineering. John Wiley & Sons, 2011.

[2] P. M. Beauchamp and J. A. Cutts, "Solar power technologies for future planetary science missions", NASA/Jet Propulsion Laboratory-Caltech, Pasadena, JPL D-10136, 2017.

[3] D. N. Micha et al., "Desenvolvimento de células solares de múltiplas junções para aplicações espaciais no laboratório de semicondutores da PUC-Rio", in VII Congresso Brasileiro de Energia Solar, Gramado, Brazil, April 2018.

[4] D. N. Micha and R. T. Silvares Junior, "The influence of solar spectrum and concentration factor on the material choice and the efficiency of multijunction solar cells", Scientific Rep., vol. 9, n.º 1, December 2019. Available: https://doi.org/10.1038/s41598-019-56457-0

[5] D. N. Micha et al., "Development of back side technology for light trapping and photon recycling in GaAs solar cells", Prog. Photovoltaics: Res. Appl., vol. 27, n.º 2, p. 163–170, October 2018. Available: https://doi.org/10.1002/pip.3076

[6] P. M. Stella, N. Mardesich, K. Edmondson, C. Fetzer and A. Boca, "Mars optimized solar cell technology (MOST)," 2008 33rd IEEE Photovoltaic Specialists Conference, San Diego, CA, USA, 2008, pp. 1-6, doi: 10.1109/PVSC.2008.4922711.

[7] P. M. Stella et al., "Multijunction Solar Cell Technology for Mars Surface Applications," 2006 IEEE 4th World Conference on Photovoltaic Energy Conference, Waikoloa, HI, USA, 2006, pp. 1907-1910, doi: 10.1109/WCPEC.2006.279869.

[8] R. M. Bunch, "Radiometry, photometry, and color", in Optical Systems Design Detection Essentials. IOP Publishing, 2021. Available: https://doi.org/10.1088/978-0-7503-2252-2ch6

[9] National Aeronautic And Space Administration. "Earth fact sheet". https://nssdc.gsfc.nasa.gov/planetary/factsheet/earthfact.html.

[10] National Aeronautic And Space Administration. "Mars fact sheet". https://nssdc.gsfc.nasa.gov/planetary/factsheet/marsfact.html.

[11] D. N. Micha and R. T. Silvares, "A self-consistent interactive model for the study of luminescence coupling in multijunction solar cells", J. Appl. Phys., vol. 130, n.º 24, pp. 243103, December 2021. Available: https://doi.org/10.1063/5.0070174

[12]I. Vurgaftman, J. R. Meyer and L. R. Ram-Mohan, "Band parameters for III–V compound semiconductors and their alloys." J. Appl. Phys. Vol. 89, p. 5815–5875, 2001.